Effect of the Number of Nucleic Acid Oligomer Charges on the Salt Dependence of Stability (ΔG°_{37}) and Melting Temperature (T_m): NLPB Analysis of Experimental Data†

Irina A. Shkel*,‡ and M. Thomas Record, Jr.‡,§

Department of Chemistry and Department of Biochemistry, University of Wisconsin−Madison, Madison, Wisconsin 53706

Received December 11, 2003; Revised Manuscript Received March 31, 2004

ABSTRACT: For nucleic acid oligomers with variable chain lengths, the salt concentration ([salt]) dependences of the denaturation temperature (T_m) and of the free energy of helix formation at 37 °C (ΔG°_{37}) are predicted using nonlinear Poisson−Boltzmann (NLPB) calculations. Analysis of experimental data reveals that the ratio of the [salt] derivative of melting temperature ($ST_m = dT_m/d \log[salt]$) to the value for a polymer with the same base composition ($ST_m/ST_{m,\infty}$) is independent of base composition but *strongly* dependent on the number of DNA charges ($|Z|$) below ∼8 bp for two-strand helices (formed from association of two complementary strands) and below ∼18 bp for hairpin helices (formed from folding of one self-complementary strand). We interpret these $ST_m/ST_{m,\infty}$ ratios in terms of the ratio of thermodynamic ion release from the oligomer (Δn_u, per charge) to that from the same oligomer embedded in polymeric DNA ($\Delta n_{u,\infty}$, per charge). Experimental values of $ST_m/ST_{m,\infty}$ and its dependence on $|Z|$ are in good agreement with NLPB predictions for a preaveraged (essential structural) model of DNA. In particular, the NLPB calculations describe the stronger $|Z|$ dependence of ST_m observed for melting of oligomeric hairpin helices than for melting of two-strand helices. These calculations predict an experimentally detectable (≥10%) difference between ST_m and $ST_{m,\infty}$ which increases strongly with decreasing length for two-strand helix lengths of <15 bp and for hairpin helix lengths of <30 bp. From NLPB values of $\Delta n_u/\Delta n_{u,\infty}$, we predict ΔG°_{37} as a function of [salt] and $|Z|$. Predictions of thermodynamic and thermal stabilities of oligomeric helices as functions of length and [salt] are consistent with and represent a significant refinement of the average oligomer salt effect currently in use in nearest neighbor stability predictions.

Nucleic acid oligomers (oligoelectrolytes) are extensively used in biophysical studies as models of polymeric nucleic acids (polyelectrolytes). Recently, DNA oligomers and other charged oligomers have been applied in microelectromechanical devices (*1*, *2*) and, by themselves or as a part of DNA−nanoparticle biocomposites, in new technologies of biocomputation (*2*) and of optical (*3*) and conductivity (*4*) sensors for high-selectivity DNA detection. All these new applications are based on the ability of charged nucleic acid oligomers to bind specifically to each other or to other charged ligands or proteins. In all these studies, the salt concentration ([salt])[1] is found to be a very important variable. For example, in emerging technological applications of DNA oligonucleotide arrays, salt concentration is used as a control variable for oligomer−oligomer hybridization processes with the aim of differentiating a target 27-base DNA oligomer (based on the anthrax lethal factor sequence) from one with a single mismatch (*4*).

Thermodynamics of processes involving nucleic acid oligomers, including conformational transitions and binding of oligocations, exhibit a strong dependence on [salt] and, in general, on the number of oligomer charges (i.e., chain length) as a consequence of Coulombic interactions. Well-characterized examples include the strong reduction relative to corresponding polymeric properties in [salt] dependences of the melting temperature ($ST_m \equiv dT_m/d \log[salt]$) of oligomeric helices, including self-complementary d(TA) hairpin helices (*5*) and duplexes from complementary strands (*6*−*8*). Figure 1 presents experimentally measured ST_m as a function of the number of DNA phosphate charges ($|Z|$) in hairpin helices (*5*, *9*−*12*) and two-strand helices (*10*), (*12*−*17*) at 0.01−0.5 M salt (1:1), where T_m is usually a strong, relatively linear function of log[salt]. Two effects are present in these experimental data: a dependence of ST_m on GC content at a fixed $|Z|$ (equivalently, fixed oligomer chain length) and a dependence of ST_m on $|Z|$ at a fixed GC content. In this study, we use the observed GC dependence of $ST_{m,\infty}$,

† This research was supported in part by NIH Grant GM47022 and in part by the University of Wisconsin−Madison.

* To whom correspondence should be addressed: Department of Chemistry, University of Wisconsin−Madison, 1101 University Ave., Madison, WI 53706-1396. Phone: (608) 262−3019. Fax: (608) 262-3453. E-mail: ishkel@wisc.edu.

‡ Department of Chemistry.

§ Department of Biochemistry.

[1] Abbreviations: [salt], salt concentration; NLPB, nonlinear Poisson−Boltzmann; ss, single-stranded; ds, double-stranded; CC, counterion condensation; GCMC, grand canonical Monte Carlo; MC, Monte Carlo; NN, nearest neighbor.

10.1021/bi036225e CCC: $27.50
Published on Web 05/08/2004

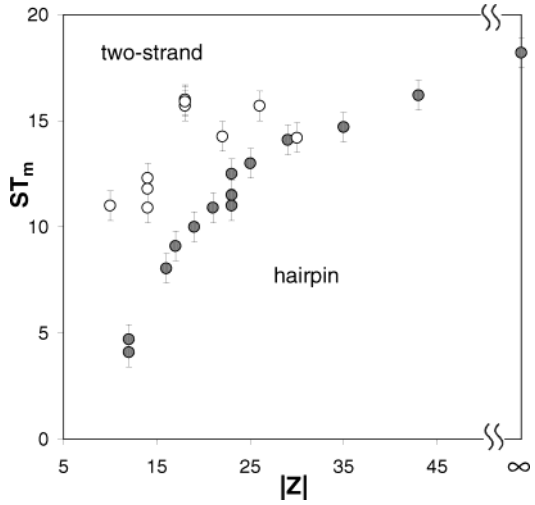

FIGURE 1: Salt concentration dependence of the transition temperature ($ST_m \equiv dT_m/d\ \log[salt]$) as a function of the number of phosphate charges $|Z|$ from hairpin melting studies (gray circles) and two-strand helix melting studies (○) presented in Table 1.

the derivative of T_m with respect to log[salt] for corresponding polymeric DNA, to separate these two effects and interpret the $|Z|$ dependence of oligomeric ST_m employing electrostatic calculations with the nonlinear Poisson−Boltzmann (NLPB) equation.

Another example is provided by the free energy of DNA duplex formation at 37 °C (ΔG°_{37}) (*7*), where the reported oligomeric $\partial\Delta G^\circ_{37}/\partial$ ln[salt], obtained as an average of [salt] dependences determined for duplexes of 4−16 bp and varying GC contents, is found to be 35% lower than its polymeric value. Commenting on the differences between poly- and oligoduplexes, the author concludes that "the nearest neighbor parameters themselves are not length-dependent but the salt dependence is length-dependent in ways that are still not fully understood". In this study, we derive expressions of practical use to predict or interpret the dependence of ΔG°_{37} of formation of two-strand and hairpin helices on the number of oligomer charges ($|Z|$) and [salt].

We test whether Coulombic theory and the preaveraged structural model of a nucleic acid oligomer are capable of predicting and interpreting these [salt] effects as a function of nucleic acid oligomer length (i.e., number of oligomer charges) and solution variables in an effort to understand the origin of differences between oligomeric and polymeric behavior. We investigate the length dependence of the thermodynamic extent of salt ion accumulation per DNA phosphate n_u,[2] rigorously defined in terms of the salt−DNA preferential interaction coefficient Γ_u (expressed per DNA phosphate) as (*19*)

$$n_u = 1 + 2\Gamma_u \tag{1}$$

using numerical NLPB calculations with a cylindrical (standard primitive) model of a nucleic acid oligomer.

The results show that at moderate [salt] (0.01−1 M) the onset of the polyelectrolyte level of ion accumulation per structural charge for a homologous series of oligomers of increasing length is determined primarily by oligomer radius, and not by the Debye length. We conclude that Coulombic end effects on average properties (such as ion accumulation) must be considered in interpretations of experimental data for nucleic acid oligomers below 1 M salt, at least for oligomers that are shorter than 10 times the oligomer radius. Coulombic end effects are always important for analysis of salt effects on processes such as fraying of helices or end binding of ligands which occurs at the ends of polymeric or oligomeric nucleic acid chains.

MODEL AND METHOD OF ANALYSIS

Salt Effects on $\Delta G^\circ_{obs,u}$ and T_m of Nucleic Acid Conformational Changes. The salt dependences of T_m ($ST_m \equiv dT_m/d\ \log[salt]$) and ΔG°_{obs} for conformational transitions of nucleic acid oligomers are related to those of the corresponding polymeric nucleic acids by (see the derivation in the Appendix)

$$\frac{ST_m}{ST_{m,\infty}} = \frac{\Delta n_u}{\Delta n_{u,\infty}} \frac{|Z|}{N_n - X} \tag{2}$$

$$\frac{\partial \Delta G^\circ_{obs,u}}{\partial\ \ln[salt]} = \frac{\Delta n_u}{\Delta n_{u,\infty}} \frac{\partial \Delta G^\circ_{obs,u,\infty}}{\partial\ \ln[salt]}, \tag{3}$$

where $\Delta G^\circ_{obs,u}$ is observed change in free energy in the transition expressed per oligomer charge, Δn_u is the stoichiometrically weighted difference between the number of thermodynamically associated ions per phosphate for product and reactant states (cf. eq 1), $|Z|$ is the number of phosphate charges, N_n is the number of nucleotides in the double-helical conformation of DNA oligomer, and X is the number of nucleotides not contributing to the reaction enthalpy (e.g., in a hairpin loop, estimated as described in the Appendix). We only consider processes without any change in the total number of nucleic acid structural charges (e.g., no protonation or deprotonation). Limiting values of ST_m, Δn_u, and $\Delta G^\circ_{obs,u}$ as $|Z| \rightarrow \infty$ are denoted with a subscript ∞. They refer to a hypothetical block polymer of the oligomeric sequence with one phosphate charge per monomer (base); though values of $ST_{m,\infty}$ and $\Delta n_{u,\infty}$ are not available for these block polymers, they are approximated from data for polymers with the same GC content as the oligomer. For polymeric DNA, ST_m is known to decrease linearly with increasing GC content (*20*, *21*). Here we use an average of the published relationships:

$$ST_{m,\infty} = 19.6(1 - 0.38 f_{GC}) \tag{4}$$

where f_{GC} is the fraction of GC base pairs.

In eqs 2 and 3, Δn_u and $\Delta n_{u,\infty}$ are expressed per phosphate charge. The number of oligomer charges $|Z|$ may be different from the number of nucleotides N_n because of the absence of phosphates on terminal nucleotides of DNA strands. In what follows, we examine the case for which $|Z| = N_n - 2$ for two-strand helices and $|Z| = N_n - 1$ for hairpin helices.

The dependence of the ion association quantity n_u on $|Z|$ is calculated by the NLPB equation as described below and expressed in the form of a linear relationship as the inverse number of oligomer phosphate charges

$$n_u = n_{u,\infty} - \frac{2\gamma}{|Z|}, \text{ for } |Z| \geq |Z|_l \tag{5}$$

[2] The subscript u here and below denotes quantities expressed per oligomer charge (i.e., per phosphate).

Table 1: Salt Dependence of Melting Temperature ($ST_m \equiv dT_m/d \log[\text{salt}]$) in Transitions of ss- and dsDNA Oligomers and Thermodynamic Extent of Ion Release Calculated from Experiments (Δn_u^{exp}) and Numerically from eq 7 at 0.15 M Salt (Δn_u^{num})[a,b]

N_n	f_{GC}	[salt] (M)	T_m (°C)	ST_m (°C)	$\Delta H°$ (kcal/mol)	$-\Delta n_u^{exp}$	$-\Delta n_u^{num}$	ref
				Hairpin Helix Melting				
18	0	0.01−0.5	40.5	8.8	42.3[c]	0.056 ± 0.006	0.062	*5*
20	0		43.5	10.0	50.3[c]	0.064 ± 0.006	0.072	
22	0		45	10.9	58.0[c]	0.072 ± 0.007	0.080	
26	0		47	13.0	73.4[c]	0.091 ± 0.009	0.092	
30	0		48	14.1	88.6[c]	0.102 ± 0.01	0.101	
36	0		50.5	14.7	112.5[c]	0.110 ± 0.01	0.111	
44	0		52	16.2	143.9[c]	0.124 ± 0.012	0.120	
poly	0		57	18.2	3.9[d]	0.157[e] ± 0.016	0.158	
13	0.31	0.01−0.1	28	4.1	24	0.022 ± 0.002	0.031[f]	*9*
13	0.62		69	4.7	39	0.032 ± 0.003	0.031[f]	
17	0.71	0.01−0.3	83	8.1	59	0.057 ± 0.006	0.055	*11*
24	0.33	0.002−0.3	55	11.5	54	0.061 ± 0.006	0.087	*12*
24	0.33	0.01−0.1	35.4	11	63.1	0.077 ± 0.008	0.087	*10*
24	0.33		44.7	12.5	61.2	0.080 ± 0.008	0.087	
				Two-Strand Helix Melting				
12	0.67	0.012−0.15	35.5	4.8	45	0.118 ± 0.01	0.114	*15*
16	0.5	0.002−0.3	58	12.3	58	0.096 ± 0.01	0.127	*12*
16	0.5	0.01−0.1	16.5	10.9	54.2	0.122 ± 0.012	0.127	*10*
16	0.5		13.9	11.8	54.9	0.136 ± 0.014	0.127	
20	0.4	0.02−0.5	43	6.9	68	0.146 ± 0.015	0.133	*14*
20	0.2	0.02−1	49.9	15.6	72.4	0.147 ± 0.015	0.133	*13*
20	0.2		45.6	16	66.5	0.142 ± 0.014	0.133	
24	0.67	0.01−0.1	53.1	6.6	90	0.134 ± 0.013	0.138	*18*
28	0.42	0.004−0.1	53.0	15.7	98	0.135 ± 0.014	0.141	*17*
32	0.67	0.015−0.115	69.4	6.2	134	0.132 ± 0.013	0.143	*16*

[a] Values of Δn_u^{exp} are evaluated from experimental measurements of T_m, ST_m, and $\Delta H°$ with eq 22. [b] The error in values of Δn_u^{num} is ±0.004. [c] Calculated from eq 26, per nucleotide value (*d*), and assumption of salt- and temperature-independent $RT_m^2/\Delta H°_{u,\infty} = 55.5$ °C. [d] Per nucleotide value of polymeric d(AT), $\Delta H°_{u,\infty}$, measured experimentally (*5*). [e] This value is used as $\Delta n_{u,\infty}^{exp}$ in normalization of experimental data of hairpin and two-strand helix melting transitions for Figure 3. [f] Calculated directly from eq 21 and not from the linear relationship of eq 7.

where the end effect parameter, γ, describes the deviation in ion accumulation and/or exclusion of an oligomer from that of the corresponding polymer and $|Z|_l$ is the minimum number of oligomer phosphate charges required for eq 5 to predict n_u within a specified accuracy. We apply this relationship to a $DNA_{ds} \rightarrow k DNA_{ss}$ oligonucleotide transition between two conformations of the nucleic acid, where k is the number of strands generated by dissociation of the double helix ($k = 1$ for hairpin helices; $k = 2$ for two-strand helices) and where the changes in ion accumulation are Δn per double-stranded molecule and Δn_u per charge

$$\Delta n = k n_{ss} - n_{ds} = \Delta n_{u,\infty}|Z| - 2(k\gamma_{ss} - \gamma_{ds}) \quad (6)$$

$$\Delta n_u = \Delta n_{u,\infty} - \frac{2(k\gamma_{ss} - \gamma_{ds})}{|Z|} \quad (7)$$

where $|Z|$ is the number of phosphate charges in the double-stranded (ds) DNA conformation and $\Delta n_{u,\infty} = n_{u,\infty,ss} - n_{u,\infty,ds}$. Equation 7 states that Δn_u differs from the polymeric value ($\Delta n_{u,\infty}$) at a given $|Z|$ by an amount which depends on both the end effect parameter (γ) and the number of the strand k.

Cylindrical Oligomer Model of a Nucleic Acid. NLPB calculations are performed with a cylindrical oligomeric model of the nucleic acid oligomer with a minimal set of important structural inputs: number of phosphate charges ($|Z|$), average axial charge separation (b) and effective radius (a). The oligomer charge is uniformly distributed along the length $|Z|b$ of the cylinder axis. The cylinder has uncharged cylindrical caps 4 Å in length [whereby the distance of closest approach of anions to the terminal charges is the same for both single-stranded (ss) and ds oligomers]. The dielectric constant of the molecular interior (D_{int}) is taken to be 2 and of molecular exterior (D_{ext}) is 78.7 (water at 25 °C). The choice of dielectric constants is consistent with previous calculations (*22*, *23*). The NLPB equation is employed as a method of calculation of ion concentration and electrostatic potential distribution, using a numerical algorithm which is similar to that employed previously (*24*) (details of numerical calculations will be published elsewhere). Numerical values of n_u are calculated as described in the Appendix (eqs 20 and 21) at 0.01, 0.05, 0.15, 0.3, 0.6, and 1 M salt (1:1) for typical structural parameters of ss- and dsDNA ($a_{ss} = 7$ Å, $a_{ds} = 9.4$ Å, $b_{ss} = 3.4$ Å, and $b_{ds} = 1.7$ Å) and lengths between 2 and 70 charges. Coefficients $n_{u,\infty}$ and γ of eq 5 are determined by a linear fit of n_u as a function of $1/|Z|$ at a sufficiently large $|Z|$.

RESULTS

Dependences of ST_m for Oligo- and Polymeric DNA on Base Composition. In this section, we test the hypothesis that the dependence of ST_m of an oligomer on GC content at a fixed [salt] is the same as that of corresponding polymer so that $ST_m/ST_{m,\infty}$ is independent of base composition. Table 1 summarizes literature values of ST_m for melting transitions of oligomeric DNA two-strand and hairpin helices. Experimental values of ST_m^{exp} in Table 1 are average values over the indicated salt range of the experimental data. Polymeric $ST_{m,\infty}$ values defined by eq 4 are also average values approximately over the same [salt] range. Values of Δn_u^{exp} for these transitions are calculated from eqs 22 and 28 of the Appendix using experimentally measured ST_m^{exp} and T_m^{exp}

Table 2: Salt Dependence of the Thermodynamic Extent of Salt Ion Accumulation per DNA Phosphate (n_u) for ss- and dsDNA Oligomers (A) and Melting Transitions (B) Predicted by NLPB Calculations for the Preaveraged Model of the Nucleic Acid Oligomer[a,b]

(A)

	ss					ds				
[salt] (M)	$\Gamma_{u,\infty}$	$n_{u,\infty}$	γ	$\|Z\|_l$	$2\gamma/n_{u,\infty}$	$\Gamma_{u,\infty}$	$n_{u,\infty}$	γ	$\|Z\|_l$	$2\gamma/n_{u,\infty}$
0[c]	−0.12	0.76				−0.06	0.88			
0.01	−0.198	0.603	1.64	12 (16)	5.44	−0.126	0.748	2.65	16 (20)	7.1
0.05	−0.235	0.53	0.92	8 (10)	3.5	−0.157	0.688	1.84	12 (16)	5.3
0.15	−0.273	0.454	0.6	5 (8)	2.64	−0.194	0.612	1.42	10 (13)	4.6
0.3	−0.301	0.398	0.46	5 (7)	2.3	−0.225	0.550	1.19	9 (12)	4.3
0.6	−0.331	0.338	0.34	4 (6)	2.0	−0.261	0.478	0.97	8 (12)	4.1
1	−0.354	0.292	0.27	4 (6)	1.85	−0.189	0.422	0.83	8 (12)	3.9
∞[d]	−0.5	0	0			−0.5	0	0		

(B)

		$dsDNA^{\|Z\|-} \rightarrow 2\ ssDNA^{\|Z\|/2-}$			$dsDNA^{\|Z\|-} \rightarrow ssDNA^{\|Z\|-}$		
[salt] (M)	$\Delta n_{u,\infty}$	$-(2\gamma_{ss} - \gamma_{ds})$	$2(2\gamma_{ss} - \gamma_{ds})/\Delta n_{u,\infty}$	$\|Z\|_l$	$-(\gamma_{ss} - \gamma_{ds})$	$2(\gamma_{ss} - \gamma_{ds})/\Delta n_{u,\infty}$	$\|Z\|_l$
0[c]	−0.120						
0.01	−0.145	−0.63	−8.6	24	0.99	13.6	24
0.05	−0.158	−0.04	≅0	16	0.92	11.6	18
0.15	−0.158	0.22	2.8	8	0.82	10.4	14
0.3	−0.152	0.27	3.5	8	0.73	9.6	14
0.6	−0.140	0.29	4.1	12	0.64	9.2	14
1	−0.130	0.29	4.4	12	0.56	8.6	12
∞[d]	0	0			0		

[a] Values of the minimum oligomer length $|Z|_l$ are calculated for the less than 10% (values in parentheses for less than 2%) deviation of numerical values of n_u from the linear relationship of eq 7. [b] The error in $\Gamma_{u,\infty}$ is ±0.001, in $n_{u,\infty}$ is ±0.002, and in $\Delta n_{u,\infty}$ is ±0.004, and the relative error in γ is less than 3%. [c] NLPB and CC limit of low [salt]. [d] Theoretical prediction for the Coulombic part in the limit of high [salt].

values and direct determinations or estimates of $\Delta H°$ (see the Appendix). Values of Δn_u^{num} are calculated from eq 7. Numerical coefficients for eqs 5 and 7 are summarized in Table 2 at six salt concentrations. Values of Δn_u^{num} at 0.15 M are presented for comparison with Δn_u^{exp} in Table 1 because all experimental data include this [salt].

Each experimental ST_m^{exp} is normalized by the corresponding polymeric $ST_{m,\infty}$ and plotted in Figure 2 as a function of the number of phosphate charges $|Z|$. Figure 2 reveals two clear trends from this normalization: $ST_m^{exp}/ST_{m,\infty}$ depends strongly on $|Z|$ for a sufficiently small $|Z|$ and the dependence of $ST_m^{exp}/ST_{m,\infty}$ on $|Z|$ is much stronger for hairpin helices than for two-strand helices. The difference between ST_m and $ST_{m,\infty}$ exceeds 20% for two-strand helix lengths of <8 bp and for hairpin helix lengths of <18 bp. Both Figures 1 and 2 provide evidence for the effect of oligomer charge $|Z|$ on ST_m, especially for hairpin helices. The normalization by $ST_{m,\infty}$ (Figure 2) separates the charge effect from the base composition effect on ST_m. Experimentally determined values of the $\Delta n_u^{exp}/\Delta n_{u,\infty}^{exp}$ ratio are plotted in Figure 3. They depend strongly on the number of oligomer charges $|Z|$ and show no significant variation with sequence, thereby supporting the assumption that $\Delta n_u/\Delta n_{u,\infty}$ is sequence-independent. $\Delta n_u^{exp}/\Delta n_{u,\infty}^{exp}$ ratios [Figure 3 (gray circles and ○)] agree within the experimental uncertainty with NLPB predictions by eqs 9 and 12 from the next section [Figure 3 (solid lines)].

Melting of Two-Strand Helices (k = 2). For melting of helices formed from two complementary strands (*10*, *12*−*18*), the process is

$$dsDNA^{|Z|-} \rightarrow 2ssDNA^{0.5|Z|-} \qquad (8)$$

From eq 7, at 0.15 M salt (1:1), we obtain the following

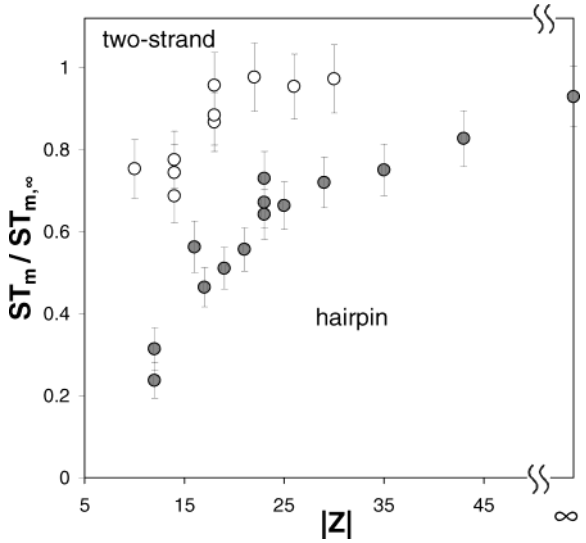

FIGURE 2: Dependence of $ST_m/ST_{m,\infty}$ of DNA hairpins (gray circles) and two-strand helices (○) on the number of oligomer phosphate charges $|Z|$. Polymeric values of $ST_{m,\infty}$ are calculated as described in Model and Method of Analysis. Error bars are estimated from the 7% uncertainty in $ST_{m,\infty}$ and the ±0.6 °C uncertainty in ST_m.

expression for Δn_u, the change in ion accumulation per nucleic acid phosphate converted from the ds to the ss state (see Table 2 for numerical coefficients) for $|Z| \geq 8$ (5 bp):

$$\frac{\Delta n_u}{\Delta n_{u,\infty}} = 1 - \frac{2.8}{|Z|} \qquad (9)$$

This expression and eq 2 predict the dependence of ST_m for denaturation of a two-strand DNA helix on the number of phosphates $|Z|$ in the two-strand form in the vicinity of 0.15 M salt [where the number of base pairs equals $0.5(|Z| + 2)$

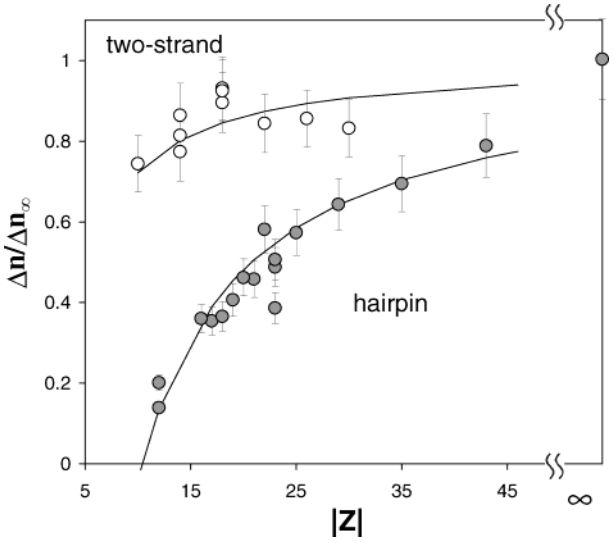

FIGURE 3: Comparison of $\Delta n_u^{exp}/\Delta n_{u,\infty}^{exp}$ calculated from Table 1 for hairpins (gray circles) and two-strand helices (○), and theoretical calculation by eqs 9 and 12 (—).

for a two-strand helix oligomer lacking one terminal phosphate on each single strand]:

$$ST_m = ST_{m,\infty}\frac{|Z| - 2.8}{|Z|} \qquad (10)$$

when $|Z| \geq 8$ nucleotides. Figure 4A compares predicted values of ST_m with experimental values of ST_m^{exp} for melting of oligomeric DNA two-strand helices with a base GC composition in the range of 20−67% measured between 0.01 and 0.3 M salt. The solid line represents the predicted dependence of ST_m on $|Z|$ calculated from eq 10 for melting of an oligomer with an average GC content for this data set (44% GC), for which base composition $ST_{m,\infty} = 16.3$ °C. Dashed lines represent the predicted behavior of ST_m for lower and upper bounds on ST_m corresponding to 20 and 67% GC DNA. Experimental points are in agreement with this prediction (the experimental uncertainty in ST_m is estimated to be ±0.6 °C as described in the next section). In addition, Figure 4A compares individual predictions of ST_m (◆) calculated with NLPB values of Δn_u^{num} and experimental T_m^{exp} and $\Delta H°$. Individual predictions of ST_m demonstrate better agreement with experimentally measured values; the standard deviation of individual predictions from experimental values of ST_m is 2 times smaller than that of average prediction. The numerical coefficients in the numerators of eqs 9 and 10 are predicted to vary strongly with [salt] for this DNA conformational transition, and are only quantitatively accurate in a small [salt] range near 0.15 M.

Melting of Hairpin Helices (k = 1). Self-complementary DNA strands of a sufficient length form hairpin helices:

$$\text{dsDNA}^{|Z|-} \rightarrow \text{ssDNA}^{|Z|-} \qquad (11)$$

In this reaction, the number of phosphates $|Z|$ is the same in the ss and ds forms of an oligomer, in contrast to melting of two-strand helices, where $|Z|$ is reduced by half upon strand separation.

The NLPB numerical prediction of Δn_u for the process of hairpin melting (*5*, *9*−*12*) in the vicinity of 0.15 M

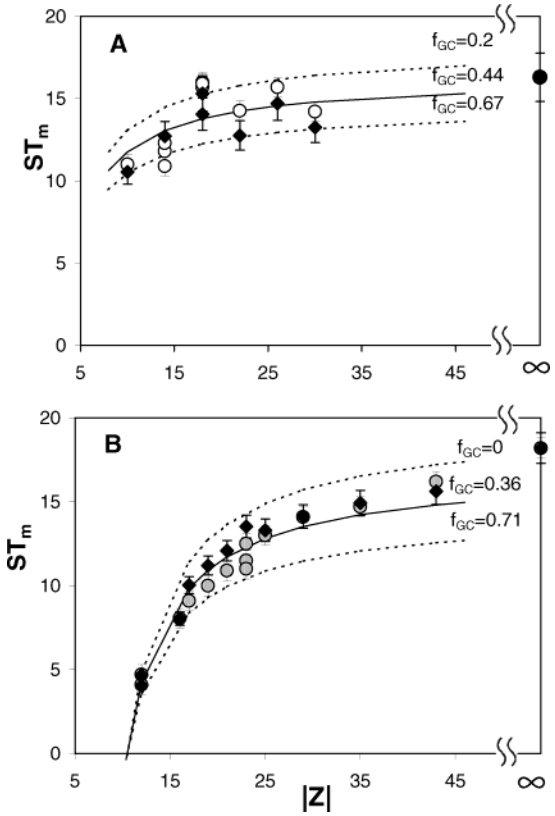

FIGURE 4: Prediction of ST_m for DNA two-strand (A) and hairpin (B) helices. (A) The solid line shows the predicted average ST_m values obtained by eq 10 for a GC content of 44%. The dotted lines are lower and upper bounds for predicted ST_m corresponding to GC contents of 20 and 67%. Empty circles are experimental values of ST_m for two-strand helices. Individual predictions of ST_m (◆) are evaluated from eqs 4 and 10. Error bars for individual predictions are estimated from the 7% experimental uncertainty in $ST_{m,\infty}$ and the numerical uncertainty in Δn and Δn_∞ given in the footnotes of Tables 1 and 2. (B) The solid line shows the predicted average ST_m values obtained with eq 13 for a GC content of 36%. Dotted lines are predictions of ST_m for GC contents of 0 and 71% for the entire set of hairpin data. Filled circles are experimental values of ST_m for hairpin helices. Individual predictions of ST_m (◆) are evaluated from eqs 4 and 13.

salt (1:1) for $|Z| \geq 13$ is

$$\frac{\Delta n_u}{\Delta n_{u,\infty}} = 1 - \frac{10.4}{|Z|} \qquad (12)$$

Comparison of eq 12 with eq 9 demonstrates a larger dependence of $\Delta n_u/\Delta n_{u,\infty}$ on $|Z|$ for unfolding or folding of hairpin helices than for two-strand helices, where the creation of two shorter denatured strands reduces the difference between Δn and $\Delta n_{u,\infty}$. For hairpin melting, the length dependence of the salt derivative ST_m is predicted from eqs 2 and 12:

$$ST_m = ST_{m,\infty}\frac{|Z| - 10.4}{|Z| - X + 1} \qquad (13)$$

where X is the number of bases in the hairpin helix which do not contribute to the enthalpy of melting. (To a first approximation, for a hairpin loop size of N_h bases, $X = N_h + 2$ (*25*); for a double hairpin, $X = N_h$.)

Comparison of experimental measurements of ST_m^{exp} and prediction from eq 13 at 0.15 M salt is presented in Figure

Table 3: Prediction of T_m and ΔG°_{37} for Helix Formation per Mole of Duplex from NLPB Calculations of Δn for Hairpin Helix Melting and Two-Strand Helix Melting[a]

[salt] (mM)	Δn^{num}_{∞}	Δn^{num}	$\Delta G^{o,exp}_{37}$ (cal/mol)	$\Delta G^{o,num}_{37}$ (cal/mol)	T^{exp}_m (°C)	$\Delta H^{\circ,exp}$ (kcal/mol)	ST^{num}_m (°C)	T^{num}_m (°C)
Hairpin Helix Melting ($N_n = 24$, from ref *12*)								
2.44			40	34.6	310.3	51.5		311.3
8.4			1060	960.4	316.1	55	10.0	316.6
10	3.34	1.36						
33.6			2220	1999	322.6	57.4	11.1	322.9
50	3.63	1.79						
100			3080	3080	328.5	53.3	12.2	328.5
150	3.63	1.99						
300			4040	4291	334.4	55.5	13.8	334.7
1000	2.99	1.87						
Two-Strand Helix Melting ($N_n = 12$, from ref *15*)								
10	1.45	1.5[b]						
12			3500	3577	296.4	44	15.1	295.1
42			4540	4539	302.4	44.3	12.3	302.5
50	1.58	1.28[b]						
150	1.58	1.14	5440	5440	308.7	47.5	10.5	308.7
300	1.52	0.98		5846			9.1	311.7
600	1.4	0.82		6191			7.6	314.3
1000	1.3	0.72	5880	6408	311.5	42.4	6.7	315.7

[a] Numerical values of ST_m, $(\partial G^\circ_{37}/RT)/(\partial \ln[\text{salt}])$, and Δn are calculated from eqs 2, 24, and 7, respectively. Polymeric [salt] dependences of melting temperature are evaluated with eq 4: $ST_{m,\infty}(0.15\text{ M}) = 17.1$ °C (for ref *12*) and $ST_{m,\infty}(0.15\text{ M}) = 14.6$ °C (for ref *15*). At salt concentrations above 0.3 M, polymeric values of the salt derivative of the melting temperature are scaled as polymeric ion release from column 2 using the assumption of salt independence of $RT_m^2/\Delta H^\circ_{u,\infty}$ (Appendix). [b] Calculated directly from eq 21 and not from the linear relationship of eq 7.

4B. T^{exp}_m and ST^{exp}_m for Elson's data are estimated from Figure 1 of ref 5 with an uncertainty in T^{exp}_m of ±0.5 °C, producing an uncertainty in ST^{exp}_m of ±0.6 °C. The solid line shows the ST_m values calculated from eq 13 with an average GC content for this data set (36% GC, $ST_{m,\infty} = 16.9$ °C). Dashed lines represent the predicted behavior of ST_m for lower and upper bounds on ST_m corresponding to 0 and 71% GC DNA. Experimental values of ST_m are in agreement with this predicted length dependence (estimated above an uncertainty in ST_m of ±0.6 °C assumed for all experimental data), including three shorter hairpins, 13-nucleotide (*9*), 17-nucleotide (*11*), and three 24-nucleotide double hairpins (*10*, *12*). Individual predictions of ST_m (◆) demonstrate better agreement with experimentally measured values; the standard deviation of individual predictions from experimental values of ST_m is 2 times smaller than that of the average prediction.

Equation 13 predicts a large reduction in the oligomeric ST_m as compared to the polymeric value. This effect is much stronger than for a two-strand helix with the same number of phosphate charges $|Z|$ at the same [salt], even though the Coulombic end effect is the same in the helical form, because of the difference in the Coulombic end effect in the denatured state. The numerical coefficients in the numerators of eqs 12 and 13 vary with [salt], although not as strongly as the corresponding coefficient for the reaction of two-strand helix melting. Figure 4B shows that eq 13 provides a prediction of the length dependence of the average ST_m within experimental uncertainty for the entire set of experimental data of oligomeric DNA transitions between 0.01 and 0.3 M.

Effect of Oligomer Length and [Salt] on the [Salt] Dependence of ΔG°_{obs} and T_m. On the basis of the calculated length dependence of n_u for ss- and ds-nucleic acids (eq 7), we integrate eqs 2 and 24 to obtain the following expression for T_m and ΔG°_{obs} of oligomeric DNA transitions as a function of [salt] and $|Z|$

$$\Delta G_{obs} = \Delta G_{obs,0} - 0.9RT[\Delta n_{u,\infty,0}|Z| - 2(k\gamma_{ss} - \gamma_{ds})_0] \ln\left(\frac{[\text{salt}]}{[\text{salt}]_0}\right) \quad (14)$$

$$T_m = T_{m,0} + ST_{m,\infty,0}\frac{|Z|}{|Z| - X + k}\left[1 - \frac{2(k\gamma_{ss} - \gamma_{ds})_0}{\Delta n_{u,\infty,0}|Z|}\right] \ln\left(\frac{[\text{salt}]}{[\text{salt}]_0}\right) \quad (15)$$

where a subscript 0 denotes values at a reference [salt]. Integration of eqs 2 and 24 is performed at constant values of γ (Table 2) and α; therefore, eqs 14 and 15 are accurate between any two consecutive [salt] in Table 2 and for oligomers longer than a specified minimum number of charges $|Z|_l$ (Table 2). Variations with [salt] of α, $\Delta n_{u,\infty}$, and $k(\gamma_{ss} - \gamma_{ds})$ are neglected in this integration because they introduce less than 10% error in $\partial\Delta G_{obs}/\partial \ln[\text{salt}]$ and ST_m between any two consecutive [salt] from Table 2, which is comparable to the experimental error in these derivatives.

Table 3 compares the prediction for T_m and ΔG°_{37} of helix formation obtained with eqs 14 and 15 with the experimentally determined values in double-hairpin (*12*) and two-strand (*15*) helix melting. The two studies are chosen from those in Table 1 because both T_m and ΔG°_{37} were determined over a wide range of [salt], from 0.008 to 0.3 M (*12*) and from 0.001 to 1 M (*15*). As the first reference [salt] we choose 0.15 M for ref *12* and 0.1 M for ref *15*. When values of ST^{num}_m and Δn^{num} are not available at a given $[\text{salt}]_0$, they are found by linear interpolation between the two closest available values. Values of T_m and ΔG°_{37} for each subsequent [salt] (both increasing and decreasing) are calculated with eqs 14 and 15. For better accuracy, average values of ST_m and Δn from each [salt] range are used for substitution in eqs 14 and 15.

DISCUSSION

Separating the Length and Sequence Dependence of ST_m. Although salt effects on the thermodynamic stability and

thermostability of poly- and oligomeric nucleic acids depend on the nucleic acid base composition (or sequence), our results indicate (Figures 2 and 3) that within the error of considered experimental data, the base composition dependence of ST_m and $\partial\Delta G^\circ_{37}/\partial$ ln[salt] is attributed to their polymeric values and the chain length dependence is attributed to $\Delta n_u/\Delta n_{u,\infty}$.

The predicted dependence of $\Delta n_u/\Delta n_{u,\infty}$ on the number of oligomer charges, $|Z|$, is a purely Coulombic effect related only to electrostatic interaction of the helical array of charges of a nucleic acid with each other and with ions in solution. It is not affected by the presence or absence of other interactions (such as the absence of a stacking interaction between bases in a hairpin loop). The Coulombic effect is influenced by the axial charge density and the radius of the looped region of the hairpin. Here we assume that phosphate charges in the hairpin loop accumulate ions to the same extent as they would in a double-helical region. The length dependence of $\Delta n_u/\Delta n_{u,\infty}$ results simply from a Coulombic end effect: charges at the oligomer ends interact with other oligomer charges in one direction, while oligomer charges in the middle interact with oligomer charges in both directions. Non-Coulombic interactions (stacking, base pairing, hydrogen bonding, etc.) are accounted for in ΔG°_{37}(1 M), in the enthalpy of reaction, ΔH°, and by the term $N_n - X$ explicitly entering eq 2.

Prediction of $\partial\Delta G^\circ_{37}/\partial$ ln[Salt] for Two-Strand Helices ($k = 2$) from NLPB Analysis at 0.15−1 M Salt. Reference *7* provides empirical expressions for the [salt] dependence of the free energy of polymeric (eq 16) and oligomeric (eq 17) two-strand helix formation between 0.02 and 1 M (with 1 M as a reference [salt])

$$\Delta G^\circ_{37,\infty} = \Delta G^\circ_{37,\infty}(1\text{ M}) - 0.175\ln[\text{salt}] - 0.20 \quad (16)$$

$$\Delta G^\circ_{37} = \Delta G^\circ_{37}(1\text{ M}) - 0.114(|Z|/2)\ln[\text{salt}] \quad (17)$$

In eq 16 for polymeric nucleic acids, values of $\Delta G^\circ_{37,\infty}$ are expressed in kilocalories per mole of base pairs. Oligomeric ΔG°_{37} values in eq 17 are expressed in kilocalories per mole of ds oligomer, obtained as a fit of experimental two-strand data on ds oligomers with 4−16 bp and with various GC contents (*7*). Here we apply eq 14 to evaluate $\Delta G^\circ_{37} - \Delta G^\circ_{37}$ (1 M). (Note that $\Delta G^\circ_{37} = -\Delta G^\circ_{obs}$ because ΔG°_{37} in nearest neighbor (NN) theory is the free energy of helix formation and ΔG°_{obs} in eqs 24 and 25 is the free energy of helix melting.)

The polymeric value of $\partial\Delta G^\circ_{37,\infty}/\partial$ ln[salt] (−0.175) from eq 16 is related to Δn_∞: $\Delta n_{u,\infty} = 0.905\partial\Delta G^\circ_{37,\infty}/\partial$ ln[salt] (obtained from eq 25 at 37 °C and after substitution of $\Delta n_\infty = \Delta n_{u,\infty}|Z|$ and $\Delta G^\circ_{obs,\infty} = -\Delta G^\circ_{37,\infty}|Z|/2$). The numerical factor of $^1/_2$ in this expression arises from conversion of $\Delta G^\circ_{37,\infty}$ per base pair to $\Delta G^\circ_{u,\infty}$ per phosphate. The experimentally observed ion release $\Delta n^{exp}_{u,\infty}$ (−0.157 ± 0.03) is in agreement with the NLPB result [$\Delta n^{num}_{u,\infty}$(0.15 M) = −0.158 ± 0.004]. In conformational transitions of nucleic acids, $\Delta n_{u,\infty}$ (from NLPB) has a broad maximum between 0.1 and 0.3 M, varying by only a few percent in this range (*26*); this explains the relative invariance of $\Delta n_{u,\infty}$ and the linearity of $T_{m,\infty}$ with respect to ln[salt] in this [salt] range. Above 0.3 M, $|\Delta n_\infty|$ decreases (from 0.158 at 0.15 M to 0.130 at 1 M) as does the predicted value of $\partial\Delta G^\circ_{37,\infty}/\partial$ ln[salt] (from 0.175 at 0.15 M to 0.144 at 1 M).

Equations 9 and 14 predict the effect of [salt] on the free energy of formation of two-strand helices in the vicinity of 0.15 M salt:

$$\frac{1}{|Z|}\frac{\partial\Delta G^\circ_{37}}{\partial\ln[\text{salt}]} = \frac{\partial\Delta G^\circ_{37,\infty}}{\partial\ln[\text{salt}]}\frac{\Delta n_u}{\Delta n_{u,\infty}} = \frac{\partial\Delta G^\circ_{37,\infty}}{\partial\ln[\text{salt}]}\left(\frac{|Z| - 2.8}{|Z|}\right)$$

In other words, in the vicinity of 0.15 M the Coulombic end effect acts to reduce the [salt] dependence of ΔG°_{37} by a factor of $(|Z| - 2.8)/|Z|$. At 1 M salt, the multiplicative factor in this expression becomes $(|Z| - 4.4)/|Z|$.

This prediction of $\Delta n_u/\Delta n_{u,\infty}$ and T_m (Table 3) overestimates experimentally observed behavior at 1 M salt (1:1), indicating that effects other than Coulombic salt effects may be significant at this [salt]. This effect may include volume and [salt]-dependent terms neglected in n_u (*27*) or specific salt effects. We tested the effect of ion size, neglected in the NLPB equation, on $\Delta n_u/\Delta n_{u,\infty}$ using the Modified Poisson−Boltzmann equation [MPB (*28*)] with an ion radius of 2 Å at 1 M salt (1:1). We found a 5−7% change in $\Delta n_{u,\infty}$ ($\Delta n^{MPB}_{u,\infty} = -0.124$) and $\gamma_{ds} - 2\gamma_{ss}$ ($\gamma^{MPB}_{ds} - 2\gamma^{MPB}_{ss} = 0.27$), resulting in a <1% change in $\Delta n_u/\Delta n_{u,\infty}$, which cannot explain the observed deviation of $\Delta G^{\circ,num}_{37}$ and ST^{num}_m from $\Delta G^{\circ,exp}_{37}$ and ST^{exp}_m at 1 M salt (Table 3).

A specific anion effect, perhaps from weak preferential (Hofmeister) interactions of Cl^- with bases in ssDNA, may be significant above 0.15 M salt (*29*). By analogy with previous work (*19*), this effect is introduced as the additional term $K_{sp}N_n$[salt], in the right-hand side of eqs 28 and 29, where the coefficient K_{sp} describes the strength of a specific anion effect with a single DNA base. We estimate K_{sp} from melting data for 6 bp (*15*) and 10 bp (*14*) two-strand helices above 0.3 M NaCl. Assuming that Coulombic contributions to ion accumulation are negligible between 2 and 5 M NaCl (*14*), we obtain a K_{sp} of 0.055 M^{-1} for the effect of NaCl on ST_m of a 10 bp two-strand helix. On the other hand, use of a K_{sp} of 0.083 M^{-1} yields agreement between predicted values of ΔG°_{37} and T_m at 1 M salt for the 6 bp helix (Figures 5 and 6) and experimental data (*15*). Predictions of ΔG°_{37} and T_m between 0.01 and 0.15 M salt are not significantly altered by this term. The apparent difference between two values of K_{sp} may result from neglecting Coulombic interactions above 1 M salt or from any dependence of K_{sp} on DNA composition. Figures 5 and 6 indicate that combination of Coulombic and specific anion effects may be sufficient to explain the [salt] dependence of T_m and ΔG°_{37} in melting of oligomeric helices.

On the basis of the corrections for specific ion effects and substituting the average values of $\partial\Delta G^\circ_{37,\infty}/(\partial$ ln[salt]) and $\Delta n_u/\Delta n_{u,\infty}$ in the [salt] range of 0.15−1 M into eq 14, we propose following the approximate expression for [salt] and charge dependence of ΔG°_{37} between 0.15 and 1 M

$$\Delta G^\circ_{37} \cong \Delta G^\circ_{37}(1\text{ M}) - 0.177(0.5|Z| - 1.8)\ln[\text{salt}] + 0.614K_{sp}(|Z| + 2)[\text{salt}] \quad (18)$$

where we use an average K_{sp} of ≅0.07 M^{-1} for Cl^- salts. Equation 18 is derived only for the salt range of 0.15−1 M. Below 0.15 M salt, it is more accurate to use eq 14. Equation 18 is written with ΔG°_{37}(1 M) as a reference point for

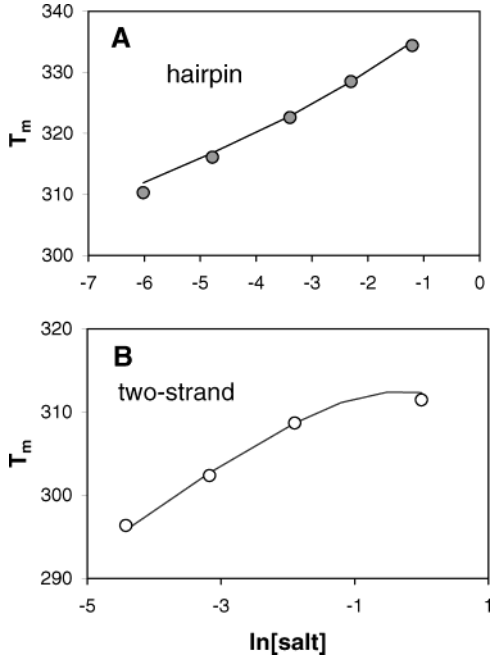

FIGURE 5: Prediction of T_m for melting of the 24-nucleotide double hairpin (*12*) (A) and the 12-nucleotide two-strand helix (*15*) (B). Circles are experimental data, and solid lines are predictions of T_m evaluated as described in the text.

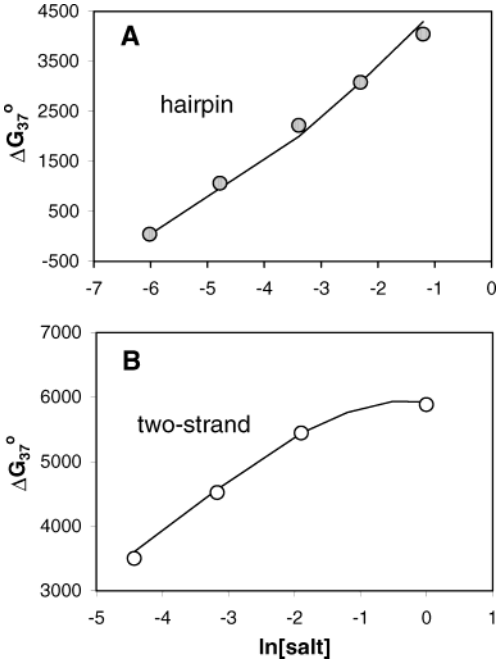

FIGURE 6: Prediction of ΔG_{37}° for melting of the 24-nucleotide double hairpin (*12*) (A) and the 12-nucleotide two-strand helix (*15*) (B). Circles are experimental data, and solid lines are predictions of ΔG_{37}° evaluated as described in the text.

application in NN theory. Such a high [salt] is also often used in DNA arrays to minimize electrostatic repulsion of two strands and optimize the hybridization conditions.

Prediction of $\partial\Delta G_{37}^{\circ}/\partial$ ln[Salt] for Hairpin Helices ($k = 1$) from NLPB Analysis at 0.15−1 M Salt. The analogous prediction of average $\partial\Delta G_{37}^{\circ}/\partial$ ln[salt] at 0.15−1 M salt for hairpin melting from NLPB analysis of the Coulombic end effect and with the empirical term for specific anion effect yields

$$\Delta G_{37}^{\circ} \cong \Delta G_{37}^{\circ}(1\text{ M}) - 0.177(0.5|Z| - 4.8)\ln[\text{salt}] + 0.614K_{sp}(|Z| + 1)[\text{salt}] \quad (19)$$

The polymeric value $\partial\Delta G_{37,\infty}^{\circ}/(\partial$ ln[salt]) for hairpin helices (eq 19) is exactly the same as that for two-strand helices (eq 18). The numerical factor relating the polymeric and oligomeric salt dependence of free energy is now

$$\frac{1}{|Z|}\frac{\partial\Delta G_{37}^{\circ}}{\partial\ln[\text{salt}]} = \frac{\partial\Delta G_{37,\infty}^{\circ}}{\partial\ln[\text{salt}]}\left(\frac{|Z| - 10.4}{|Z|}\right)$$

at 0.15 M and

$$\frac{1}{|Z|}\frac{\partial\Delta G_{37}^{\circ}}{\partial\ln[\text{salt}]} = \frac{\partial\Delta G_{37,\infty}^{\circ}}{\partial\ln[\text{salt}]}\left(\frac{|Z| - 8.6}{|Z|}\right)$$

at 1 M. Substituting the average values of $\Delta n_u/\Delta n_{u,\infty}$ in the [salt] range of 0.15−1 M into eq 14, we obtain eq 19. Because $\Delta n_u/\Delta n_{u,\infty}$ is less [salt]-dependent for hairpin helices than for two-strand helices (see the next section), eq 19 should be applicable over a broader [salt] range (from 0.01 to 1 M).

Predicted Difference between Salt Effects on Oligomeric and Polymeric Nucleic Acids. There are two distinctions in the predicted salt dependences between polymeric and oligomeric nucleic acids. The first is the reduction in the oligomeric Δn_u (and, consequently, in ST_m and $\partial\Delta G_{obs}^{\circ}/(\partial$ ln[salt]); the second is the stronger [salt] dependence of oligomeric Δn_u (and, consequently, nonlinearity in T_m and ΔG_{obs}° with respect to log[salt]). The first effect is especially evident in hairpin melting, where the oligomeric slope $\partial\Delta G_{37}^{\circ}/(\partial$ ln[salt]) ($\propto\Delta n$) is roughly half the polymeric value over the entire [salt] range (0.01−1 M) and slowly increases as [salt] increases. For two-strand oligomeric helices, Δn_u is more similar to $\Delta n_{u,\infty}$ and exhibits the opposite trend with respect to [salt], being the same as the polymeric value at 0.01 M, only 25% smaller than the polymeric value at 0.05 and 0.15 M salt, but only 50% of the polymeric value at 1 M. The nonlinearity of T_m and ΔG_{obs}° is especially expressed for the shortest two-strand helices. For an $N_n = 12$ ($|Z| = 10$) two-strand helix, numerical data from Table 3 predict a 2 times smaller ST_m at 1 M than at 0.15 M salt, which is consistent with experimental measurements (*15*). For hairpin helices, the nonlinearity is predicted to increase with decreasing salt concentration, which is also observed in experimental data (Figures 5 and 6). The differences between oligomeric and polymeric [salt] dependences increase with a decrease in $|Z|$. The predicted Δn_u is 74% of the polymeric value for the shortest two-strand helix (*15*) and 20% of the polymeric value for the shortest hairpin helix (*9*).

Coulombic End Effect; Experimental Results and Theoretical Approaches. Various theoretical descriptions of the effect of [salt] on nucleic acid processes involve calculation of the [salt] derivative of the electrostatic free energy of reactants and products (obtained by integration and/or charging) (*30*−*37*). Alternatively, Record and co-workers (*19*, *25*, *27*, *38*) developed a direct thermodynamic analysis connecting the [salt] derivative of thermodynamic characteristics of a charged biopolymer/oligomer process to the change in the thermodynamic extent of ion association Δn for the products and reactants (eqs 22−25 of the Appendix).

We call the differences in the [salt] dependence of thermodynamic parameters between oligomers and polymers Coulombic end effects and relate them to the effects of oligomer ends on ion distribution around an oligomer. These effects are illustrated by an approximately trapezoidal distribution of surface potential and local counterion concentration along a cylindrical model of a long nucleic acid oligomer obtained from Monte Carlo (MC) (*39*) and NLPB (*22*) calculations. The surface counterion concentration exhibits the polymeric value in the interior region but decreases almost linearly in two terminal regions, each of which constitutes 20 charges for dsDNA and 10 charges for ssDNA at 1−12 mM salt (*39*). Similarly, the surface potential distribution is trapezoidal for sufficiently long oligomers; each terminal region spans 14 charges at 0.001 M salt and 10 charges at 0.1 M salt for dsDNA (*22*). Thus, at the end of the oligomer (or polymer), the surface counterion concentration is lower than in the interior of the polymer (or sufficiently long oligomer), and consequently, n_u is smaller. Investigation of the dependence of n_u on $|Z|$ and [salt] was performed for a cylindrical model of ds- and ssDNA by grand canonical Monte Carlo (GCMC) simulations at 0.002−0.0135 M salt (1:1) (*25*). GCMC predictions of oligomer n_u, and, consequently, the log[salt] dependence of the oligomer melting temperature, are consistent with the very different behaviors of hairpin and two-strand helix melting data in the range of 0.002−0.0135 M salt (1:1), which is at the lower end of the usual experimental range (typically, 0.01−0.5 M). The salt dependence of the free energy of duplex formation (ΔG°_{37}) is mostly studied between 0.1 and 1 M salt, because of the choice of ΔG°_{37}(1 M) as a reference state in NN theory. Our results provide an extension of the treatment of Coulombic end effects to higher [salt] necessary to explain experimental data above 0.01 M salt.

Some other theoretical analyses have reached a different conclusion, namely, that thermodynamic characteristics of even short oligomers exhibit polyelectrolyte-like behavior at moderate [salt]. The existence of this controversy is clearly revealed in the recent authoritative treatise on nucleic acids (*40*), where both interpretations are presented (one in Chapter 8 and the other in Chapter 11). In some analyses based on Debye−Huckel approximation (*41*), the BBGKY hierarchy of equations (*42*), or counterion condensation (CC) theory (*43*), the Debye length is predicted to be the characteristic length which determines the onset of polymeric behavior of oligomers. By this approach, a 20 bp dsDNA oligomer is sufficiently long to be in the polyelectrolyte limit at 0.1 M salt. For example, CC (*43*) and Monte Carlo (MC) (*44*, *45*) analyses, both using local, distance-dependent dielectric parameters and either the cylindrical model (*46*) or a structurally detailed model of DNA, predict only a few percent difference in number of accumulated conterions per phosphate for the polyion and 20 bp oligomer at 0.1 M. However, the data in Figure 1 and other experimental data on molecular (*47*) and thermodynamic (*48*, *49*) consequences of salt−nucleic acid interactions show clear differences in salt effects between the oligomer and polymer even at 0.1−0.3 M salt and are consistent with our calculations from Table 2A, indicating that the extent of salt ion association per DNA phosphate for a 20 bp dsDNA at 0.15 M salt is only 87% of the polymeric value. Our calculation provides a means of evaluating a length characterizing the consequences of the Coulombic end effect on the thermodynamic extent of ion accumulation for DNA oligomers. It follows from eq 5 that the $4\gamma/n_{u,\infty}$ value from Table 2 represents the length at which the extent of salt ion accumulation per DNA phosphate is half the polymeric value ($n_u/n_{u,\infty} = 0.5$). It is evident from Table 2 that this length decreases gradually with increasing [salt] in the range of 0.01−1 M, not scaling with the Debye length. Our unpublished NLPB calculations with a range of *a* and *b* for the preaveraged DNA oligomer model indicate that this length is approximately proportional to *a* and weakly dependent on *b* above 0.01 M salt (1:1).

CONCLUSIONS

Explicit expressions for the thermodynamic extent of salt ion accumulation by a DNA oligomer as a functions of oligomer length (number of phosphate charges) are obtained between 0.01 and 1 M salt (1:1) for structural parameters of ss- and dsDNA. These expressions describe the sequence-independent contribution of oligomer charges to the [salt] dependence of its thermodynamic parameters. Combined with the sequence-dependent enthalpy of the reaction and the polymeric salt derivative of the melting temperature, they provide prediction of the [salt] derivative of the oligomer melting temperature in good agreement with experiments. Our calculations predict not only the average oligomeric [salt] dependence (Figure 4) but also differential effects on Δn and ST_m in the experimental [salt] range (Figures 5 and 6) for the two most common conformational transitions of DNA oligomers, and we conclude that the preaveraged DNA oligomer model (with the set of structural parameters specified above) is sufficient to describe experimental [salt] dependences of nucleic acid oligomeric transitions. On the basis of the obtained length dependence of the thermodynamic degree of ion accumulation, we propose expressions for [salt] and length dependence of the free energy ΔG°_{37} of formation of the two-strand helix and of the hairpin helix which agree with experimentally observable dependence of ΔG°_{37} on salt concentration.

ACKNOWLEDGMENT

We thank Dr. H. Ni for preliminary NLPB calculations.

APPENDIX

The thermodynamic extent of ion accumulation, n, is the thermodynamic quantity which characterizes the consequences of salt cation accumulation and salt anion exclusion in the vicinity of the nucleic acid; *n* is related to the salt−nucleic acid preferential interaction coefficient (Donnan coefficient) Γ by

$$n \equiv |Z| + 2\Gamma \tag{20}$$

where *Z* is the total nucleic acid charge. Equation 20 can be rewritten per nucleic acid phosphate as eq 1 in the text. Expressed per phosphate, n_u is the same as the quantity called ψ by Record *et al.* (*50*). For polymeric dsDNA at low (limiting law) [salt], $\Gamma_u = -0.06$ and $n_u = 0.88$ (*19*). The ion−oligomer preferential interaction coefficient Γ is related to integrals over space of the local deficit in concentration of an excluded co-ion (C_-) as compared to its "bulk" value (*27*, *51*):

$$\Gamma = \int_V [C_-(r) - C_-^{\text{bulk}}]\, dV \quad (21)$$

The co-ion distribution for calculations of n is evaluated from the mean field approximation $C_- = C_-^{\text{bulk}} e^{-y}$, where y is the magnitude of the reduced electrostatic potential.

The preferential interaction coefficient is related to the [salt] dependence of thermodynamic properties of a conformational transition such as the equilibrium constant and melting temperature (*19*, *24*, *25*). In derivation of eqs 2 and 3, we use (*19*)

$$ST_m = -2.303\alpha \frac{2RT_m^2}{\Delta H^o} \Delta\Gamma = -2.303\alpha \frac{RT_m^2}{\Delta H^o} \Delta n \quad (22)$$

$$ST_{m,\infty} = -2.303\alpha \frac{RT_{m,\infty}^2}{\Delta H^\circ_\infty} \Delta n_\infty \quad (23)$$

$$\frac{\partial \Delta G_{obs}}{\partial \ln[\text{salt}]} = -\alpha RT \Delta n \quad (24)$$

$$\frac{\partial \Delta G_{obs,\infty}}{\partial \ln[\text{salt}]} = -\alpha RT \Delta n_\infty \quad (25)$$

where oligomeric values ΔH° and Δn are expressed per molecule in the ds form and the relation $\alpha \equiv 1 + \partial \ln \gamma_\pm / \partial \ln[\text{salt}]$ accounts for the nonideality of the salt ion (in the [salt] range of 0.01−1 M, $\alpha \cong 0.9$ for NaCl). Polymeric values in eqs 22−25 refer to a polymer composed of a repeated oligomer sequence with all phosphate charges present. ΔH°_∞ and Δn_∞ are expressed per N_n nucleotides of the polymer. The following relationships for oligo- and polymeric values (per molecule and per charge) are assumed

$$\Delta H^\circ(T_m) = \Delta H^\circ_{u,\infty}(T_m)(N_n - X) \quad (26)$$

$$\Delta H^\circ_\infty(T_{m,\infty}) = \Delta H^\circ_{u,\infty}(T_{m,\infty}) N_n \quad (27)$$

$$\Delta n = \Delta n_u |Z| \quad (28)$$

$$\Delta n_\infty = \Delta n_{u,\infty} N_n \quad (29)$$

where X is the number of nucleotides in the nucleic acid helix not contributing to the reaction enthalpy. We use an X of 2 for two-strand helices (because $0.5N_n$ base pairs have $0.5N_n - 1$ stacking interactions in a linear duplex); likewise, $X = N_h + 2$ for one-strand hairpin helices with loops of N_h nucleotides. However, $X = 8$ for double hairpins with two loops of four nucleotides each, because no stacking interactions are lost at the interior of the double hairpin.

In DNA transitions, $\Delta H^\circ_{u,\infty}$ is a strong function of $T_{m,\infty}$ because of the large heat capacity change (*52*). Extant data indicate that $RT_m^2/\Delta H^\circ_{u,\infty}$ is not significantly [salt]- and temperature-dependent in polymeric (*53*, *24*) and oligomeric (*54*, *55*) DNA transitions. Substituting eqs 26−29 into eqs 22−25, dividing eq 22 by eq 23 and eq 24 by eq 25, and assuming the constancy of $RT_m^2/\Delta H^\circ_{u,\infty}$, we obtain eqs 2 and 3. The same assumption is used for evaluation of transition enthalpy for ref 5 in Table 1 and polymeric values of salt derivative of melting temperature at high salt in Table 3.

Polymeric Values of ST_m and Δn. Somewhat different expressions for the dependence of the polymer derivative $ST_{m,\infty}$ on GC content exist in the literature. Frank-Kamenetskii (*20*) generalized the [salt] dependence of the melting temperature of four polymeric DNAs with GC contents between 0.24 and 0.72 measured at 0.01−0.3 M salt as $ST_m = 18.3(1 - 0.38 f_{GC})$. Blake *et al*. (*21*) obtained larger values of ST_m at any GC content at 0.075−1 M salt: from 21 °C for poly-AT to 13.2 °C for poly-GC (*21*). However, the results of Blake and Frank-Kamenetskii yield the same ST_m(0% GC)/ST_m(100% GC) ratio of 1.6. Experimental measurements at a fixed GC content show that ST_m is approximately constant between 0.01 and 0.3 M salt (1:1) but decreases above 0.3 M salt. For example, for poly-d(AT) (*5*), an ST_m value of 22.5 °C is obtained using the two low-[salt] experimental determinations (0.01 and 0.06 M), while the 15% smaller ST_m value of 18.2 °C is obtained from data at three [salt] (0.01, 0.06, and 0.5 M). Thus, for normalization of experimental data in Figure 2, we choose a polymeric $ST_{m,\infty}$ value of $19.6(1 - 0.38 f_{GC})$ °C as an average between the values of Blake (*21*) and Frank-Kamenetskii (*20*). The resulting uncertainty in $ST_{m,\infty}$ is approximately ±7%, comparable to the experimental uncertainty in the determination of $ST_{m,\infty}$ and its variation with [salt].

In the numerical calculation of $\Delta n_u/\Delta n_{u,\infty}$ as a function of $|Z|$, we use polymeric structural quantities of a nucleic acid model (*a* and *b*) obtained by Bond *et al*. (*24*) from fitting of experimental measurements on T2 phage DNA dialysis and B-DNA melting transitions. The GC content of polymeric DNA in these experiments is in the range of 30−50%. Thus, the NLPB $\Delta n_{u,\infty}$ value of −0.158 from Table 2 at 0.15 M corresponds to such a GC content. This also agrees with the sequence dependence of $\Delta n_{u,\infty}$, which we estimated with eq 23 of this work from Table 1 of Blake *et al*. (*21*), where 0% GC yields a $\Delta n_{u,\infty}$ of −0.18 and 100% GC yields a $\Delta n_{u,\infty}$ of −0.12. DNA oligomers from two examples of the [salt] dependence of ΔG°_{37} and T_m in Figures 5 and 6 have similar GC content; that of the 24-nucleotide double hairpin (*12*) is 33% and that of the 12-nucleotide two-strand helix (*15*) 50%.

Coulombic End Effects in Ion Accumulation. For sufficiently long oligomers, the differences between polymeric and oligomeric preferential interaction coefficients $\Gamma_{g,u}$ (counterion, $\Gamma_{g,u} = 1 + \Gamma_u$), $\Gamma_{n,u}$ (co-ion, $\Gamma_{n,u} \equiv \Gamma_u$), and the thermodynamic degree of ion association n_u follow a linear dependence on the inverse number of oligomer charges (see eq 1)

$$\Gamma_{g,u} - \Gamma_{g,u,\infty} = \Gamma_u - \Gamma_{u,\infty} = -\frac{\gamma}{|Z|} \quad (30)$$

Because of the electroneutrality condition ($\Gamma_{g,u} = 1 + \Gamma_{n,u}$), we need to know only one Γ to calculate another one, and thermodynamic quantities such as the thermodynamic degree of ion association ($n = \Gamma_g + \Gamma_n = 2\Gamma_g - |Z| = |Z| + 2\Gamma_n$), which determines the [salt] dependence of experimentally observable quantities (eqs 2 and 3). On a per molecule basis, counterion accumulation and coin exclusion are described by (multiplying eq 30 by $|Z|$)

$$\Gamma_g = \Gamma_{g,\infty} - \gamma \quad (31)$$

$$\Gamma_n = \Gamma_{n,\infty} - \gamma \quad (32)$$

For a molecule with a non-zero net charge, $\Gamma_g > 0$, $\Gamma_n < 0$,

and $\Gamma_g + \Gamma_n > 0$, the last inequality meaning that the net effect is always an accumulation of the number of ions near a charged molecule. The end effect parameter γ characterizes the decrease in counterion accumulation (eq 31), the increase in co-ion exclusion (eq 32), and the net decrease in the per charge thermodynamic extent of ion association (eq 5) of an oligomer relative to the corresponding polymer. Table 2 provides values of $\Gamma_{u,\infty}$, $n_{u,\infty}$, and γ for ss- and dsDNA oligomers at several salt concentrations.

Onset of the Polymeric Behavior in Conformational Transitions. For melting of two-strand helices, the relative difference between oligomeric and polymeric ion release obtained from eq 7 is

$$\left|\frac{\Delta n - \Delta n_\infty}{\Delta n_\infty}\right| = \left|\frac{2(\gamma_{ds} - 2\gamma_{ss})}{\Delta n_{u,\infty}|Z|}\right| \qquad (33)$$

For melting of two-strand helices at 0.15 M salt, using the fitting parameters in Table 2, we predict that Δn differs from Δn_∞ by more than 10% for lengths of $\leq$28 (i.e., 15 bp). The same length characterizes the approach to the polymeric limit of ST_m for this reaction (compare eqs 9 and 10). For two-strand helices, $\gamma_{ds} - 2\gamma_{ss}$ varies strongly with [salt], indicating that ST_m and ΔG°_{obs} are less linear functions of ln[salt] for two-strand helices than for polymers. The value of $\gamma_{ds} - 2\gamma_{ss}$ changes sign at $\sim$0.05 M [consistent with MC calculations (*25*), where $\gamma_{ds} - 2\gamma_{ss}$ is negative below 0.013 M]. If studied in the vicinity of 0.05 M salt, the difference between Δn and Δn_∞ for melting of two-strand helices is predicted to be reduced from that predicted at 0.15 M salt.

For hairpin melting, the relative difference between oligomeric and polymeric ion release is expressed as

$$\left|\frac{\Delta n - \Delta n_\infty}{\Delta n_\infty}\right| = \frac{2(\gamma_{ds} - \gamma_{ss})}{\Delta n_{u,\infty}|Z|}. \qquad (34)$$

A more than 10% difference for hairpins between Δn and Δn_∞ predicted for lengths of $\leq$100 charges ($\sim$50 bp) should be observed in studies of ΔG°_{obs} versus [salt]. However, ST_m is predicted to be more similar to the polymer value at any chain length. The relative difference between the oligomeric and polymeric ST_m exceeds 10% for oligomers shorter than 30 bp. The difference in polymeric and oligomeric Δn is more pronounced for hairpin helices than for two-strand helices with the same base composition and number of charges. In contrast with melting of two-strand helices, the difference $\Delta n - \Delta n_\infty$ for hairpin helices shows very weak dependence on [salt] and decreases as [salt] increases (Table 2).

REFERENCES

1. Niemeyer, C. M. (2000) Self-assembled nanostructures based on DNA: toward the development of nanobiotechnology, *Curr. Opin. Chem. Biol. 4*, 609−618.
2. Bashir, R. (2001) DNA-mediated artificial nanobiostructures: state of the art and future directions, *Superlattices Microstruct. 29* (1), 1−16.
3. Storhoff, J. J., Lazarides, A. A., Mucic, R. C., Mirkin, C. A., Letsinger, R. L., and Schatz, G. C. (2000) What controls the optical properties of DNA-linked gold nanoparticle assemblies? *J. Am. Chem. Soc. 122* (19), 4640−4650.
4. Park, S.-J., Taton, T. A., and Mirkin, C. A. (2002) Array-based electrical detection of DNA with nanoparticle probes, *Science 295* (5559), 1503−1506.
5. Elson, E. L., Scheffler, I. E., and Baldwin, R. L. (1970) Helix formation by d(TA) oligomers. III. Electrostatic effects, *J. Mol. Biol. 54*, 401−415.
6. SantaLucia, J., Jr., Allawi, H., and Seneviratne, P. A. (1996) Improved nearest-neighbor parameters for predicting DNA duplex stability, *Biochemistry 35*, 3555−3562.
7. SantaLucia, J. (1998) A unified view of polymer, dumbbell, and oligonucleotide DNA nearest-neighbor thermodynamics, *Proc. Natl. Acad. Sci. U.S.A. 95*, 1460−1465.
8. Owczarzy, R., Vallone, P. M., Gallo, F. J., Paner, T. M., Lane, M. J., and Benight, A. S. (1997) Predicting sequence-dependent melting stability of short duplex DNA oligomers, *Biopolymers 44*, 217−239.
9. Rentzeperis, D., Kharakoz, D. P., and Marky, L. A. (1991) Coupling of sequential transitions in a DNA double hairpin: energetics, ion binding, and hydration, *Biochemistry 30*, 6276−6283.
10. Rentzeperis, D., Ho, J., and Marky, L. A. (1993) Contribution of loops and nicks to the formation of DNA dumbbells: melting behavior and ligand-binding, *Biochemistry 32*, 2564−2572.
11. Xodo, L. E., Manzini, G., Quadrifoglio, F., van der Marel, G. A., and van Boom, J. H. (1986) Thermodynamic behavior of the heptadecadeoxynucleotide d(CGCGCGTTTTTCGCGCG) forming B and Z hairpins in aqueous solution, *Nucleic Acids Res. 14*, 5389−5398.
12. Erie, D., Sinha, N., Olson, W., Jones, R., and Breslauer, K. (1987) A dumbell-shaped, double-hairpin structure of DNA: a thermodynamic investigation, *Biochemistry 26*, 7150−7159.
13. Park, Y. W., and Breslauer, K. J. (1991) A spectroscopic and calorimetric study of the melting behaviors of a bent and a normal DNA duplex: $[D(GA_4T_4C)]_2$ versus $[D(GT_4A_4C)]_2$, *Proc. Natl. Acad. Sci. U.S.A. 88*, 1551−1555.
14. Tomac, S., Sarkar, M., Ratilainen, T., Wittung, P., Nielsen, P. E., Norden, B., and Graslund, A. (1996) Ionic effects on the stability and conformation of peptide nucleic acid complexes, *J. Am. Chem. Soc. 118*, 5544−5552.
15. Williams, A. P., Longfellow, C. E., Freier, S. M., Kierzek, R., and Turner, D. H. (1989) Laser temperature-jump, spectroscopic, and thermodynamic study of salt effects on duplex formation by dGCATGC, *Biochemistry 28*, 4283−4291.
16. Sheardy, R. D., Levine, N., Marotta, S., Suh, D., and Chaires, J. B. (1994) A thermodynamic investigation of the melting of B−Z junction forming DNA oligomer, *Biochemistry 33*, 1385−1391.
17. Quartin, R. S., and Wetmur, J. G. (1989) Effect of ionic-strength on the hybridization of oligodeoxynucleotides with reduced charges due to methylphosphonate linkages to unmodified oligodeoxynucleotides containing the complementary sequence, *Biochemistry 28*, 1040−1047.
18. Marky, L. A., Blumenfeld, K. S., Kozlowski, S., and Breslauer, K. J. (1983) Salt-dependent conformational transitions in the self-complementary deoxydodecanucleotide d(CGCAATTCGCG): evidence for hairpin formation, *Biopolymers 22*, 1247−1257.
19. Record, M. T., Jr., Zhang, W., and Anderson, C. F. (1998) Analysis of effects of salts and uncharged solutes on protein and nucleic acid equilibria and processes: a practical guide to recognizing and interpreting polyelectrolyte effects, Hofmeister effects, and osmotic effects of salts, *Adv. Protein Chem. 51*, 281−353.
20. Frank-Kamenetskii, M. D. (1971) Simplification of the empirical relationship between melting temperature of DNA, its GC content and concentration of sodium ions in solution, *Biopolymers 10*, 2623−2624.
21. Blake, R. D., Bizzaro, J. W., Blake, J. D., Day, G. R., Delcourt, S. G., Knowles, J., Marx, K. A., and SantaLucia, J., Jr. (1999) Statistical mechanical simulation of polymeric DNA melting with MELTSIM, *Bioinformatics 15*, 370−375.
22. Allison, S. A. (1994) End effects in electrostatic potentials of cylinders: models for DNA fragments, *J. Phys. Chem. 98*, 12091−12096.
23. Sharp, K. A. (1995) Polyelectrolyte electrostatics: salt dependence, entropic, and enthalpic contributions to free-energy in the nonlinear Poisson−Boltzmann model, *Biopolymers 36*, 227−243.
24. Bond, J. P., Anderson, C. F., and Record, M. T., Jr. (1994) Conformational transitions of duplex and triplex nucleic acid helices: thermodynamic analysis of effects of salt concentration on stability using preferential interaction coefficients, *Biophys. J. 67*, 825−836.
25. Olmsted, M. C., Anderson, C. F., and Record, M. T., Jr. (1991) Importance of oligoelectrolyte end effects for the thermodynamics

of conformational transitions of nucleic acid oligomers: a grand canonical Monte Carlo analysis, *Biopolymers 31*, 1593−1604.
26. Shkel, I. A., Tsodikov, O. V., and Record, M. T., Jr. (2002) Asymptotic solution of the cylindrical nonlinear Poisson−Boltzmann equation at low salt concentration: analytic expressions for surface potential and preferential interaction coefficient, *Proc. Natl. Acad. Sci. U.S.A. 99* (5), 2597−2602.
27. Anderson, C. F., and Record, M. T., Jr. (1993) The salt-dependence of oligoion-polyion binding: a thermodynamic description based on preferential interaction coefficients, *J. Phys. Chem. 97*, 7116−7126.
28. Borukhov, I., Andelman, D., and Orland, H. (2000) Adsorption of large ions from an electrolyte solution: a modified Poisson−Boltzmann equation, *Electrochim. Acta 46*, 221−229.
29. Hamaguchi, K., and Geiduschek, E. P. (1962) The effect of electrolytes on the stability of the deoxyribonucleate helix, *J. Am. Chem. Soc. 84*, 1329−1338.
30. Misra, V. K., Sharp, K. A., Friedman, R. A., and Honig, B. (1994) Salt effects on ligand-DNA binding: minor-groove binding antibiotics, *J. Mol. Biol. 238*, 245−263.
31. Misra, V. K., Sharp, K. A., Friedman, R. A., and Honig, B. (1994) Salt effects on protein-DNA interactions: The Lambda-CI repressor and EcoRI endonuclease, *J. Mol. Biol. 238*, 264−280.
32. Sharp, K. A. (1995) Salt effect on polyelectrolyte-ligand binding: comparison of Poisson−Boltzmann, and Limiting Law/Counterion Binding models, *Biopolymers 36*, 245−262.
33. Sharp, K. A., and Honig, B. (1990) Calculating total electrostatic energies with the nonlinear Poisson−Boltzmann equation, *J. Phys. Chem. 94*, 7684−7692.
34. Beveridge, D. L., and McConnell, K. J. (2000) Nucleic acids: theory and computer simulation, Y2K, *Curr. Opin. Struct. Biol. 10* (2), 182−196.
35. Abascal, A. L. F., and Montoro, J. C. G. (2000) Computer simulation results for the free-energy difference between B-DNA and Z-DNA, *J. Phys.: Condens. Matter 12* (8A), A327−A332.
36. Kollman, P. A., Massova, I., Reyes, C., Kuhn, B., Huo, S. H., Chong, L., Lee, M., Lee, T., Duan, Y., Wang, W., Donini, O., Cieplak, P., Srinivasan, J., Case, D. A., and Cheatham, T. E. (2000) Calculating structures and free energies of complex molecules: combining molecular mechanics and continuum models, *Acc. Chem. Res. 33* (12), 889−897.
37. Stigter, D., and Dill, K. A. (1996) Binding of ionic ligands to polyelectrolytes, *Biophys. J. 71*, 2064−2074.
38. Olmsted, M. C., Bond, J. P., Anderson, C. F., and Record, M. T., Jr. (1995) GCMC molecular and thermodynamic predictions of ion effects on binding of an oligocation (L^{8+}) to the center of DNA oligomers, *Biophys. J. 68*, 634−647.
39. Olmsted, M. C., Anderson, C. F., and Record, M. T., Jr. (1989) Monte Carlo description of oligoelectrolyte properties of DNA oligomers: range of the end effect and the approach of molecular and thermodynamic properties to the polyelectrolyte limits, *Proc. Natl. Acad. Sci. U.S.A. 86*, 7766−7770.
40. Bloomfied, V. A., Crothers, D. M., and Tinoco, I., Jr. (2000) *Nucleic Acids, Structure, Properties, and Functions*, University Science Books, Sausalito, CA.
41. Skolnick, J., and Grimmelmann, E. K. (1980) A preliminary examination of end effect in polyelectrolyte theory: the potential of a line segment of charge, *Macromolecules 13*, 335−338.
42. Woodbury, C. P., Jr., and Ramanathan, G. V. (1982) End effect in polyelectrolytes by the Mayer cluster integral approach, *Macromolecules 15*, 82−86.
43. Manning, G. S., and Mohanty, U. (1997) Counterion condensation on ionic oligomers, *Physica A 247*, 196−204.
44. Jayaram, B., Swaminathan, S., Beveridge, D. L., Sharp, K., and Honig, B. (1990) Monte Carlo simulation studies on the structure of the counterion atmosphere of B-DNA. Variations on the primitive dielectric model, *Macromolecules 23*, 3156−3165.
45. Young, M. A., Jayaram, B., and Beveridge, D. L. (1997) Intrusion of counterions into the spine of hydration in the minor groove of B-DNA: fractional occupancy of electronegative pockets, *J. Am. Chem. Soc. 119*, 59−69.
46. Fenley, M. O., Manning, G. S., and Olson, W. K. (1990) Approach to the limit of counterion condensation, *Biopolymers 30*, 1191−1203.
47. Stein, V. M., Bond, J. P., Capp, M. W., Anderson, C. F., and Record, M. T., Jr. (1995) Importance of coulombic end effects on cation accumulation near oligoelectrolyte B-DNA: a demonstration using ^{23}Na NMR, *Biophys. J. 68*, 1063−1072.
48. Zhang, W., Bond, J. P., Anderson, C. F., Lohman, T. M., and Record, M. T., Jr. (1996) Large electrostatic differences in the binding energetics of a cationic peptide to oligomeric and polymeric DNA, *Proc. Natl. Acad. Sci. U.S.A. 93*, 2511−2516.
49. Zhang, W., Ni, H., Capp, M. W., Anderson, C. F., Lohman, T. M., and Record, M. T., Jr. (1999) The importance of coulombic end effects: experimental characterization of the effects of oligonucleotide flanking charges on the strength and salt-dependence of oligocation (L^{8+}) binding to single-stranded DNA oligomers, *Biophys. J. 76*, 1008−1017.
50. Record, M. T., Jr., Lohman, T. M., and de Haseth, P. (1976) Ion effects on ligand-nucleic acid interactions, *J. Mol. Biol. 107*, 145−158.
51. Ni, H., Anderson, C. F., and Record, M. T., Jr. (1999) Characterization of thermodynamic consequences of cation (M^{2+}, M^{+}) ion accumulation and anion (X^{-}) exclusion in mixed-salt solutions of polyanionic DNA using Monte Carlo and Poisson−Boltzmann calculations of ion-polyion preferential interaction coefficients, *J. Phys. Chem. 103*, 3489−3504.
52. Holbrook, J. A., Capp, M. W., Saecker, R. M., and Record, M. T., Jr. (1999) Enthalpy and heat capacity changes for formation of an oligomeric DNA duplex: Interpretation in terms of coupled processes of formation and association of single-stranded helices, *Biochemistry 38*, 8409−8422.
53. Record, M. T., Jr., Anderson, C. F., and Lohman, T. M. (1978) Thermodynamic analysis of ion effects on the binding and conformational equilibria of proteins and nucleic acids: the roles of ion association or release, screening, and ion effects on water activity, *Q. Rev. Biophys. 11*, 103−178.
54. Nakano, S., Fujimoto, M., Hara, H., and Sugimoto, N. (1999) Nucleic acid duplex stability: influence of base composition on cation effects, *Nucleic Acids Res. 27*, 2957−2965.
55. Rouzina, I., and Bloomfield, V. A. (1999) Heat capacity effects on the melting of DNA. 2. Analysis of nearest-neighbor base pair effects, *Biophys. J. 77*, 3252−3255.

BI036225E